

Autoresonant Excitation of Antiproton Plasmas

G. B. Andresen,¹ M. D. Ashkezari,² M. Baquero-Ruiz,³ W. Bertsche,⁴ P. D. Bowe,¹ E. Butler,⁴ P. T. Carpenter,⁵ C. L. Cesar,⁶ S. Chapman,³ M. Charlton,⁴ J. Fajans,³ T. Friesen,⁷ M. C. Fujiwara,⁸ D. R. Gill,⁸ J. S. Hangst,¹ W. N. Hardy,⁹ M. E. Hayden,² A. J. Humphries,⁴ J. L. Hurt,⁵ R. Hydromako,⁷ S. Jonsell,¹⁰ N. Madsen,⁴ S. Menary,¹¹ P. Nolan,¹² K. Olchanski,⁸ A. Olin,⁸ A. Povilus,³ P. Pusa,¹² F. Robicheaux,⁵ E. Sarid,¹³ D. M. Silveira,¹⁴ C. So,³ J. W. Storey,⁸ R. I. Thompson,⁷ D. P. van der Werf,⁴ J. S. Wurtele,^{3,15} and Y. Yamazaki^{14,16}

(ALPHA Collaboration)

¹*Department of Physics and Astronomy, Aarhus University, DK-8000 Aarhus C, Denmark*

²*Department of Physics, Simon Fraser University, Burnaby British Columbia, Canada V5A 1S6*

³*Department of Physics, University of California at Berkeley, Berkeley, California 94720-7300, USA*

⁴*Department of Physics, Swansea University, Swansea SA2 8PP, United Kingdom*

⁵*Department of Physics, Auburn University, Auburn, Alabama 36849-5311, USA*

⁶*Instituto de Física, Universidade Federal do Rio de Janeiro, Rio de Janeiro 21941-972, Brazil*

⁷*Department of Physics and Astronomy, University of Calgary, Calgary Alberta, Canada T2N 1N4*

⁸*TRIUMF, 4004 Wesbrook Mall, Vancouver British Columbia, Canada V6T 2A3*

⁹*Department of Physics and Astronomy, University of British Columbia, Vancouver British Columbia, Canada V6T 1Z4*

¹⁰*Fysikum, Stockholm University, SE-10691, Stockholm, Sweden*

¹¹*Department of Physics and Astronomy, York University, Toronto, Ontario, M3J 1P3, Canada*

¹²*Department of Physics, University of Liverpool, Liverpool L69 7ZE, United Kingdom*

¹³*Department of Physics, NRCN-Nuclear Research Center Negev, Beer Sheva, IL-84190, Israel*

¹⁴*Atomic Physics Laboratory, RIKEN, Saitama 351-0198, Japan*

¹⁵*Lawrence Berkeley National Laboratory, Berkeley, California 94720, USA*

¹⁶*Graduate School of Arts and Sciences, University of Tokyo, Tokyo 153-8902, Japan*

(Received 6 November 2010; published 14 January 2011)

We demonstrate controllable excitation of the center-of-mass longitudinal motion of a thermal antiproton plasma using a swept-frequency autoresonant drive. When the plasma is cold, dense, and highly collective in nature, we observe that the entire system behaves as a single-particle nonlinear oscillator, as predicted by a recent theory. In contrast, only a fraction of the antiprotons in a warm plasma can be similarly excited. Antihydrogen was produced and trapped by using this technique to drive antiprotons into a positron plasma, thereby initiating atomic recombination.

DOI: 10.1103/PhysRevLett.106.025002

PACS numbers: 52.27.Jt, 52.35.Mw

Oscillators subjected to a drive with a swept frequency can become phase locked to the drive; when this happens, the oscillator's amplitude can be controlled by varying the applied frequency. This phenomenon, called autoresonance, occurs in a variety of dynamical systems from plasma modes [1] to orbital dynamics [2]. Nonlinear oscillators can be controlled with autoresonance when one is ignorant of the oscillator's state, a fact exploited in applications from controlling Josephson junctions [3] to mass spectrometers [4]. This Letter describes the dynamics behind the autoresonant drive that we recently used to inject antiprotons into a positron plasma, thereby forming antihydrogen that we trapped [5].

Autoresonant (AR) control requires that systems (typically uncoupled nonlinear oscillators) possess an anharmonic potential with a monotonic relationship between their response frequency and amplitude. Here we study the autoresonant excitation of a thermally broadened pure antiproton plasma. Because the total potential that results

from the vacuum and plasma self-electric fields has a nonmonotonic relationship between amplitude and frequency, test particles will not respond autoresonantly. Furthermore, only a subset of thermally broadened, uncoupled test particles in the vacuum potential would have an autoresonant response. Yet we find that a charged plasma *can* behave as a single particle under autoresonant excitation despite its self-fields and thermal distribution. To our knowledge, this is the first direct confirmation of a theory developed by Barth *et al.* that claims that the repulsive self-forces cause a charged plasma to stay coherent under the autoresonance drive [6].

This Letter compares the behavior of the plasma to a single-particle oscillator of charge $-e$ and mass m , confined on the z axis in an electrostatic potential with a time-varying drive electric field E_d of the form: $\Phi = -\Phi_0[1 - \cos(kz)] - E_d z \cos(\int \omega dt)$, where Φ_0 , k , and E_d are parameters found by fitting to the actual potentials used in our measurements. Defining $\theta = kz$, \bar{e} to be a

normalized drive amplitude, and allowing the drive frequency ω to be time dependent with a sweep (chirp) rate magnitude α , the equation of motion is:

$$\ddot{\theta} + \omega_0^2 \sin\theta = \bar{\epsilon} \cos(\omega_i t - \alpha t^2/2). \quad (1)$$

This is the same equation as that of a uniformly driven, nonlinear pendulum with a linear (small-amplitude) oscillation frequency of $\omega_0 = \sqrt{ek^2\Phi_0/m}$.

On application of a *fixed* drive frequency ($\alpha = 0$), the amplitude of this oscillator beats in time, never coming to equilibrium. However, if the drive starts at an initial frequency $\omega_i > \omega_0$ and sweeps past ω_0 to a final frequency ω_f , the oscillator can phase lock to the drive and will adjust its nonlinear frequency to match that of the drive. At a sufficiently high drive amplitude, this process will be independent of the initial conditions of the oscillator [2]. In this way, the final energy U_f of the oscillator can be chosen by ω_f through the oscillator's energy-frequency relationship. This is an autoresonant drive.

The “particle” in the actual experiment is the center-of-mass longitudinal motion of an antiproton plasma. As the dynamics of this system are governed by a many-body equation of motion [6], it is not obvious that this system's behavior can be reduced to that of a single particle.

All measurements were conducted in the ALPHA apparatus, located at the Antiproton Decelerator at CERN. ALPHA contains a minimum-B trap designed for the production and trapping of neutral antihydrogen [7] and uses Penning-Malmberg traps to catch and mix its charged constituents: antiprotons and positrons. Preparation of the antiproton plasmas followed the methods described in [8], and left the antiprotons in the potential shown in Fig. 1, in which all experiments occur.

We destructively measure the antiproton number by lowering one side of the confining potential, thereby allowing the antiprotons to escape and annihilate on the end of the trap. We count the annihilation products during this “dump” with scintillators. The two plasma conditions

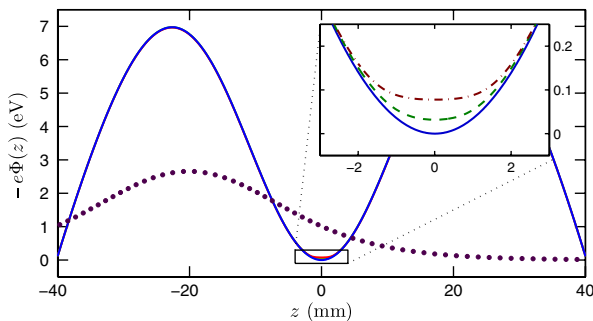


FIG. 1 (color online). On-axis ($r = 0$) potentials used in this experiment. Solid blue line, vacuum potential. Dotted line, typical drive potential ($\bar{\epsilon}/2\pi \sim 1.8 \times 10^9 \text{ s}^{-2}$ scaled $\times 100$). Inset: Total potential for the plasma ($T_{\parallel} = 150 \text{ K}$) with 15 000 (green dashed line) [$n(0, 0) \sim 6 \times 10^{12} \text{ m}^{-3}$] and 50 000 (red dotted-dashed line) antiprotons [$n(0, 0) \sim 1 \times 10^{13} \text{ m}^{-3}$].

discussed here had approximately 15 000 and 50 000 antiprotons each, although these numbers fluctuated ($\pm 30\%$). We also imaged the radial profile of the dumped plasmas and found that in both cases their average diameter was $\sim 1.6 \text{ mm}$ [9].

The annihilation times and the potential as a function of time during a dump are used to determine the approximate longitudinal energy distribution function $f(U)dU$ of the plasma. By assuming single-particle dynamics in a uniform longitudinal magnetic field and ignoring radial effects, the longitudinal energy of an antiproton is:

$$U = \frac{1}{2}mv_z^2(z) - e[\Phi(z) - \Phi(0)]. \quad (2)$$

The energy a particle has when it escapes differs from its initial energy because the dump process performs work on it. However, if a particle's longitudinal action $J = \oint mv_z dz$ is adiabatically conserved, we can equate $J(t_e)$ to $J(U_0)$, and relate its escape time t_e to its energy U_0 in the well before the dump. The dumps are slow enough to dynamically preserve J in our trap, but fast compared to the antiproton-antiproton collision rate [10]. By ignoring the plasma potential and radial effects, we introduce energy errors ($< 15 \text{ mV}$) that are much smaller than the mean energies discussed here ($> 1 \text{ V}$). All particle distributions presented here are calculated this way.

When the plasma is in thermal equilibrium, its longitudinal temperature T_{\parallel} can be determined by fitting an exponential to the high-energy tail of the longitudinal energy distribution, a method which can be largely insensitive to the plasma's self-fields [8,11]. The “cold” antiproton plasmas discussed here had temperatures in the range of (150–300) K. From the particle number, radial profile and temperature, we can calculate the plasma equilibrium density $n(r, z)$, and total potential (Fig. 1) [12].

We find the relationship of a particle energy U to a response (bounce) frequency ω_b in the potential by solving for the time τ it takes a particle to traverse the well:

$$\frac{\pi}{\omega_b(U)} = \tau(U) = \int_{z_l}^{z_r} \frac{dz}{|v_z|}, \quad (3)$$

where v_z and the left and right turning points z_l and z_r are solved from Eq. (2) for a given potential Φ . Figure 2 plots $U(\omega_b)$, for the potentials shown in Fig. 1.

We applied a drive that chirped from a frequency ω_i that was 2.5% above ω_0 to various final frequencies ω_f 's at a fixed $\alpha(2\pi \times 60 \text{ MHz s}^{-1})$. The resultant energy distributions were measured with 10 ms dumps performed 2 ms after the drive. As shown in Fig. 2, the mean energy of each distribution agrees with $U(\omega_f)$ calculated from Eq. (3), indicating that the bounce frequency of the plasma matched the drive frequency. This implies that the plasma response was phase locked to the drive.

Figure 3 shows a decrease in the mean U of distributions measured at different times after applying the same drive to similar plasmas. After the excitation, parallel energy

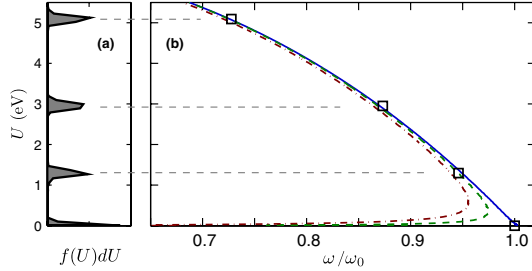


FIG. 2 (color online). Energy versus frequency measurements and calculations (frequencies normalized to $\omega_0/2\pi = 410$ kHz). (a) Distributions of ~ 15000 antiprotons driven to different final frequencies. (b) $U(\omega_b)$ calculated from Eq. (3) for the vacuum potential (solid blue line); total potential with 15000 (green dashed line) and 50000 (red dotted-dashed line) antiprotons (see Fig. 1). The open squares denote the mean U of each distribution plotted against its final drive frequency.

redistributes itself via collisions and can change to perpendicular motion or be lost through “evaporation” of high-energy particles out of the well [8,13]. Based on the measurements, we see that the single-particle assumption is valid for the 10 ms dumps used in the measurements.

One feature of autoresonantly driven systems is the existence of a critical drive amplitude $\bar{\epsilon}_c$ that scales as a distinctive $\alpha^{3/4}$ power law [14]. Specifically for oscillators obeying Eq. (1), the threshold is [2]:

$$\bar{\epsilon}_c = 8\sqrt{\omega_0}\left(\frac{\alpha}{3}\right)^{3/4}. \quad (4)$$

Above this threshold, the oscillator will lock to the drive, and the amplitude will follow the drive frequency; below the threshold, the oscillator will not lock to the drive.

This threshold is derived by modeling the phase difference between oscillator and drive as the coordinate of a “pseudoparticle” in a “pseudopotential.” Phase locking requires confinement of the pseudoparticle in a well of the pseudopotential, with a perfect phase lock corresponding to a stationary pseudoparticle. Generally, however, the pseudoparticle oscillates around one minimum of the

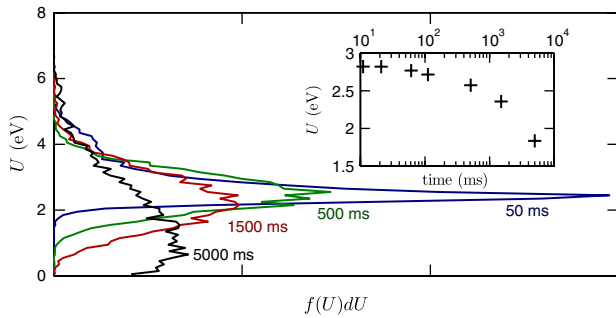


FIG. 3 (color online). Plot of the time evolution of the longitudinal distribution $f(U)dU$ for plasmas with ~ 50000 antiprotons excited with an autoresonant drive. Inset: Their mean longitudinal energy as a function of the time between the autoresonant drive and the energy measurement dump.

pseudopotential, manifesting as a modulation of the amplitude of the real system. Near the threshold, if α is too large or $\bar{\epsilon}$ too small, the pseudopotential well will become so shallow over the course of the sweep that the pseudoparticle will escape. Thereafter, no phase lock exists and the system’s energy will remain roughly constant, even as the drive continues [2].

Experimentally, we determined the autoresonance threshold in our system by driving the plasma at different amplitudes while holding ω_i , ω_f , and α constant. The threshold amplitude $\bar{\epsilon}_c$ is the value that causes the plasma’s mean energy to rise sharply. Figure 4(a) shows the data used to measure the threshold at $\alpha/2\pi \sim 200$ MHz s $^{-1}$. A curve of $\bar{\epsilon}_c$ as a function of α is shown in Fig. 4(b), and adheres to the scaling of Eq. (4).

We compared the threshold measurements with calculations for a single particle following Eq. (1) and found that the data agrees with the simulation after a uniform reduction of the simulation $\bar{\epsilon}$ by $\sim 20\%$ (consistent with an uncertainty in our estimate of the coupling between the drive electronics and the electrode); the blue curve in Fig. 4(a) includes this correction factor, and coincides with the measurements. The shape of the simulation curve is governed by details of the pseudoparticle oscillations present in the time evolution of the oscillator. In measurements of the energy after the drive, they influence the slow rise in final energy before the jump at the threshold and the fluctuations after $\bar{\epsilon}_c$. The measured data, in matching the calculations, are consistent with a pseudoparticle oscillation of the driven plasma.

These results strongly indicate that the cold plasma behaves as a single-particle oscillator under an autoresonance drive. We find, however, that a hot plasma does not respond as a single particle. We heated the cold plasma to

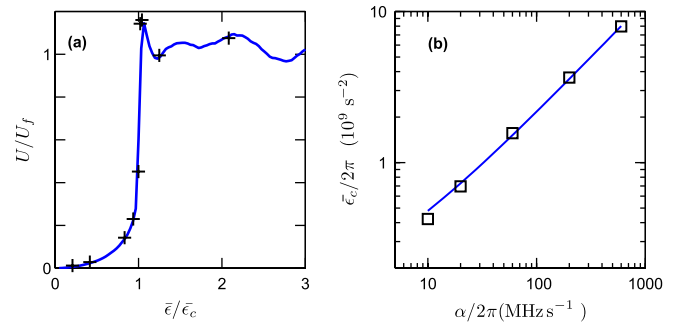


FIG. 4 (color online). Chirp and drive amplitude threshold measurements on 15000 antiprotons. (a) Amplitude threshold measurement for fixed drive parameters ($\alpha/2\pi = 200$ MHz/s, $\omega_i/2\pi = 420$ kHz, $\omega_f/2\pi = 360$ kHz), with longitudinal energy U normalized to $U_f \sim 2.9$ eV. Plus signs denote mean energy of final distributions plotted against their drive amplitude and normalized to scale the threshold to 1. The solid blue line denotes the single oscillator final energy calculated as a function of drive amplitude, similarly scaled. (b) The open squares denote measured $\bar{\epsilon}_c$ for a given chirp rate α . Scaling law (solid blue line) $\alpha^{3/4}$ [Eq. (4)] fit to the data.

$T \sim 1,800$ K by applying a strong drive near ω_0 and waited 25 s after the heating to allow for thermalization before applying the AR drive. We measured the capture threshold in the manner described above. We found that, while it started following the drive at approximately $\bar{\epsilon}_c$ for the equivalent cold plasma, the hot plasma split into two distinct populations: one that followed the drive and another that remained at low energy (Fig. 5). Increasing the amplitude captured more antiprotons.

This behavior is consistent with the model proposed in [6], where it is shown that a thermal plasma will have an $\bar{\epsilon}_c$ that scales as $\alpha^{3/4}$. In the case of a high temperature and/or low density, the threshold is broad because the plasma phase space filaments during the excitation and only a fraction of the plasma (monotonically increasing with $\bar{\epsilon}$) is captured by the drive. The model further predicts that increasing the density actually narrows the transition, because the repulsive self-fields cause the plasma to act as a single particle.

Though our plasmas are not modeled exactly in [6], their behaviors follow the expected trend of the theory. Barth *et al.* define a parameter $\eta^2 = \omega_p^2/\omega_0^2$ which quantifies the importance of the self-field of the plasma ($\omega_p = \sqrt{ne^2/m\epsilon_0}$ is the plasma frequency). For instance, they find that, for a plasma with $T_{\parallel} \sim 2,300$ K, η^2 must be greater than ~ 4 to behave like a single particle. Our hot plasma, with $\eta^2 \sim 0.5$, has a fractional response while our cold plasma, with $\eta^2 \sim 1.6$, behaved as a single particle. Though the comparison of η^2 should be made at the same temperatures, we expect collective effects to play a more important role in our cold plasma because its Debye length was shorter than any of its spatial dimensions, while it is longer in the case of the hot plasma [15]. We assessed the threshold behavior without collective effects for our plasmas by solving Eq. (1) for thermal

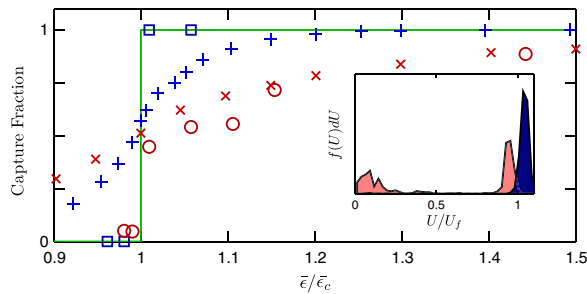


FIG. 5 (color online). Plot of the fraction of plasma that follows the autoresonant drive ($\alpha/2\pi = 60$ MHz s $^{-1}$, $\omega_i/2\pi = 420$ kHz, $\omega_f/2\pi = 360$ kHz). Cold plasma (open squares) and hot plasma (open circles) of 15 000 antiprotons. Solid green line denotes the expected fraction for a single oscillator ($T_{\parallel} = 0$ K). Blue plus signs denote calculations for an ensemble of cold oscillators ($T_{\parallel} = 150$ K). Red crosses denote calculations for an ensemble of hot oscillators ($T_{\parallel} = 1,800$ K). Inset: Distribution functions of a heated (pink [light gray]) and an unheated (blue [dark gray]) plasma after the drive ($\bar{\epsilon}/\bar{\epsilon}_c \sim 1.05$).

ensembles (at our plasma temperatures) of noninteracting particles, and determined the capture fraction for $\bar{\epsilon}$'s around $\bar{\epsilon}_c$. Figure 5 shows that this calculation, lacking self-interactions, does not predict the sharp transition at $\bar{\epsilon}_c$ that we observe for the cold plasma.

In conclusion, we have demonstrated the controlled autoresonant excitation of the mean longitudinal energy of a thermal antiproton plasma. A cold, dense plasma behaves like a single-particle oscillator, while a warm, tenuous plasma filaments under the drive, displaying a broad autoresonance threshold. This behavior is consistent with a recently published model [6].

In this Letter, we have discussed finite excitation of the plasma; by extending the sweep to lower frequencies, the antiprotons can be driven out of their well and directly into a confined positron plasma [16]. These unconfined antiprotons lose phase lock to the drive, pass through confined positrons and form antihydrogen. Many previously used methods for mixing antiprotons with positrons produced antihydrogen with too much kinetic energy to be trapped (typical traps cannot hold antiatoms with kinetic energies more than $\sim 5 \times 10^{-5}$ eV [7]). For example in [17], antiprotons were launched into the positrons by tipping them over a several eV barrier and produced antihydrogen measurably too warm to trap. In [18], antiprotons were heated over a few eV barrier into positrons with a fixed-frequency drive. In both cases, antiprotons entered the positrons with an excess of energy: either an initial excess of U or significant transverse energy gained from collisional energy redistribution; both reduce the likelihood of forming trappable antihydrogen [13]. In contrast, autoresonance injects the antiprotons into the positrons with little excess longitudinal energy, and if done sufficiently and quickly, with minimal increase in the antiprotons' original transverse energy. Once the drive parameters were tuned to those reported in [5], we found that autoresonant injection was reproducible in the face of fluctuations ($\sim 10\%$) in the number and radial profile of the initial antiproton and positron plasmas.

This work was supported by CNPq, FINEP/RENAFAE (Brazil), ISF (Israel), MEXT (Japan), FNU (Denmark), VR (Sweden), NSERC, NRC/TRIUMF, AIF, FQRNT (Canada), DOE, NSF (USA), and EPSRC, the Royal Society and the Leverhulme Trust (UK).

- [1] W. Bertsche, J. Fajans, and L. Friedland, *Phys. Rev. Lett.*, **91**, 265003 (2003).
- [2] J. Fajans and L. Friedland, *Am. J. Phys.*, **69**, 1096 (2001).
- [3] O. Naaman, J. Aumentado, L. Friedland, J. S. Wurtele, and I. Siddiqi, *Phys. Rev. Lett.*, **101**, 117005 (2008).
- [4] A. V. Ermakov and B. J. Hinch, *Rev. Sci. Instrum.* **81**, 013107 (2010).
- [5] G. B. Andresen *et al.* (ALPHA Collaboration), *Nature (London)* **468**, 673 (2010).
- [6] I. Barth, L. Friedland, E. Sarid, and A. G. Shagalov, *Phys. Rev. Lett.*, **103**, 155001 (2009).

- [7] W. Bertsche *et al.*, *Nucl. Instrum. Methods* **566**, 746 (2006).
- [8] G. B. Andresen *et al.* (ALPHA Collaboration) *Phys. Rev. Lett.*, **105**, 013003 (2010).
- [9] G. B. Andresen *et al.* (ALPHA Collaboration) *Rev. Sci. Instrum.* **80**, 123701 (2009).
- [10] F. F. Chen, *Introduction to Plasma Physics and Controlled Fusion Volume 1: Plasma Physics* (Plenum Press, New York, 1984), 2nd ed..
- [11] D. L. Eggleston, C. F. Driscoll, B. R. Beck, A. W. Hyatt, and J. H. Malmberg, *Phys. Fluids B* **4**, 3432 (1992).
- [12] S. A. Prasad and T. M. Oneil, *Phys. Fluids* **22**, 278 (1979).
- [13] C. A. Ordonez and D. L. Weathers, *Phys. Plasmas* **15**, 083504 (2008).
- [14] J. Fajans, E. Gilson, and L. Friedland, *Phys. Rev. Lett.* **82**, 4444 (1999).
- [15] C. Hansen and J. Fajans, *Phys. Rev. Lett.* **74**, 4209 (1995).
- [16] G. Andresen *et al.* (ALPHA Collaboration), *Phys. Lett. B* **695**, 95 (2011).
- [17] N. Madsen *et al.* (ATHENA Collaboration), *Phys. Rev. Lett.* **94**, 033403 (2005).
- [18] G. Gabrielse *et al.* (ATRAP Collaboration), *Phys. Rev. Lett.* **89**, 233401 (2002).